CELL BIOCHEMISTRY & FUNCTION

The fucose-specific lectin from Aspergillus niger ANL possesses anti-cancer activity, inducing the intrinsic apoptosis pathway in hepatocellular and colon cancer cells

Journal:	*Cell Biochemistry & Function*
Manuscript ID	Draft
Wiley - Manuscript type:	Research Article
Date Submitted by the Author:	n/a
Complete List of Authors:	Jagadeesh, Narasimhappagari Belur, Shivakumar Campbell, Barry. ; University of Liverpool, Department of Infection & Microbiomes, Inamdar, Shashikala; Karnatak University Dharwad, Biochemistry
Keywords:	Aspergillus niger lectin,, apoptosis,, cell cycle arrest,, alpha-fetoprotein,, lectin-ELISA
Abstract:	The L-fucose-specific lectin from Aspergillus niger (ANL), is examined by studying interaction with hepatocellular and colon cancer cells and evaluating its anti-cancer and diagnostic potential. ANL strongly bound to HepG2 and HT-29 cells which are effectively blocked with L-fucose and mucin. ANL increased hypodiploidy and decreased HepG2 cells in G0-G1 phase. ANL increased apoptosis in both HepG2 and HT-29 cells via enhancing ROS, altering MMP and activating intrinsic pathway. Immunoblotting confirmed time-dependent elevation of cytochrome c, caspase-9 and active caspase-3. Immunohistochemistry and development of an ANL-anti-AFP sandwich ELISA to quantify AFP in HCC patients confirmed diagnostic potential of ANL.

The fucose-specific lectin from *Aspergillus niger* ANL possesses anti-cancer activity, inducing the intrinsic apoptosis pathway in hepatocellular and colon cancer cells

ANL as anticancer agent

Narasimhappagari Jagadeesh[1], Shivakumar Belur[1], Barry J. Campbell[2], Shashikala R. Inamdar[1,*]

[1]Department of Studies in Biochemistry, Karnatak University, Dharwad-580003, India

[2]Department of Infection & Microbiomes, University of Liverpool, Liverpool, L69 3GE, UK

*Corresponding author. Tel.: +91 836 2215243; Fax +91 836 2747884

E-mail address: srinamdar2009@gmail.com

Acknowledgements:

SRI thanks the Council of Scientific & Industrial Research (CSIR, No. 27 (0350))/19/EMR-II dated 17th May 2019) and N Jagadeesh thanks the CSIR for fellowship under CSIR-SRF (No. 09/101(0056)/2019/EMR-I). We acknowledge Dr Vijay kumar Jhalakhi KCTRI, Hubli for providing HCC serum samples.

Abstract

The L-fucose-specific lectin from *Aspergillus niger* (ANL), is examined by studying interaction with hepatocellular and colon cancer cells and evaluating its anti-cancer and diagnostic potential. ANL strongly bound to HepG2 and HT-29 cells which are effectively blocked with L-fucose and mucin. ANL increased hypodiploidy and decreased HepG2 cells in G_0-G_1 phase. ANL increased apoptosis in both HepG2 and HT-29 cells via enhancing ROS, altering MMP and activating intrinsic pathway. Immunoblotting confirmed time-dependent elevation of cytochrome c, caspase-9 and active caspase-3. Immunohistochemistry and development of an ANL-anti-AFP sandwich ELISA to quantify AFP in HCC patients confirmed diagnostic potential of ANL.

KEYWORDS

Aspergillus niger lectin, apoptosis, cell cycle arrest, alpha-fetoprotein, lectin-ELISA

1. Introduction

Tumour cells are known for expressing different glycan profiles on their cell-surface compared to normal or non-transformed cells. Expression of altered cancer specific glycans on cancer cells is an important pathophysiological condition observed in many cancers which serves as an important cancer biomarker (1). These glycans are known to play an important role in cancer cell proliferation, cell invasion, cancer metastasis and angiogenesis and the role of glycans in these various processes has been well established. Lectins considering their unique fine sugar specificity can bind differentially to these glycans and hence can serve as cancer diagnostic agents. Expression of oncofoetal gene epitopes expressed on tumour cells has been manifested in malignant transformation and also some of them have known to be released in to the serum which serves as biomarkers (2). Many serum glycoproteins and cell-surface membrane receptors are observed known to be highly fucosylated in gastrointestinal cancers, including hepatocellular

carcinoma, pancreatic carcinoma and colon adenocarcinoma which is an important diagnostic marker (3). Differential expression of fucosyltransferases in transformed cells eventually results in increased fucosylation patterns seen in various cancers which can act as specific cancer biomarkers (4).

Alterations of both *N*- and *O*-linked glycans have been observed in many glycoproteins expressed on cancer cell surface or in the serum which serves as cancer markers (5). Many serum glycoproteins, like alpha-fetoprotein (AFP) and haptoglobin, are known to express altered *N*-glycans especially fucosylated *N*-glycans in gastrointestinal cancer, both present in abundance on the cell surface, and released into the serum during malignant transformation (6).

Serum AFP, a well-established tumour marker that is produced in hepatocellular carcinomas (HCC), has an abundance of fucose epitopes (7). Many of these specific glycans are considered as disease markers and are targets for diagnosis as well as for anti-cancers. Identification of aberrant glycosylation or glycans can be achieved by specific carbohydrate-binding proteins like lectins. Lectins, especially fucose-specific lectins, due to their sugar recognition property have been commonly used to monitor changes in fucosylation of plasma glycoproteins, such as AFP, the most reliable and widely used tumor marker for the diagnosis of hepatocellular carcinoma. Enzyme-linked immunosorbent assay (ELISA) employing an anti-AFP antibody and a fucose-specific lectin is a powerful tool for quantifying elevated levels of aberrantly glycosylated AFP in the serum, for clinical purposes (8, 9). Hence, fucose-specific lectins such as *Lens culinaris* agglutinin (LCA) and *Aspergillus oryzae* lectin (AOL) and *Cephalosporium curvulum* (CSL) are gaining clinical significance (10). Recently, we described a fucose-specific lectin from pathogenic fungus *Aspergillus niger*, ANL, with specificity towards L-fucose, fetuin, asialofetuin and porcine gastric mucin (11). ANL showed potent growth inhibitory activity on human PANC-

1 pancreatic epithelial cancer cells (11), known to overexpress fucose and Lewis antigens on secreted mucins and on cell-surface *N*-glycans (12,13). Considering these results, and the specificity of ANL towards L-fucose and cancer-related mucins, also shown to be highly expressed in hepatocellular carcinoma (HCC) and colorectal cancer (CRC) (5), this prompted us in the present study to evaluate the interaction and activity of ANL on HepG2 and HT-29 cancer cell-lines. ANL shows strong binding to both these cell-lines and exerts significant anti-cancer activity, enhancing cytotoxicity via arrest of the cell cycle, increasing ROS and there by activating cellular apoptosis involving the intrinsic pathway leading to cell death. ANL also shows differential binding to normal and cancerous colon tissues and is an effective tool in detecting tumour marker AFP in patient serum, with significantly higher sensitivity compared to LCA, a well-known currently used fucose-specific lectin. Hence, ANL has promising clinical potential in cancer diagnostics.

2. Materials and Methods

For cell culture, Dulbecco's Modified Eagle's Medium (DMEM) and foetal bovine serum (FBS) were obtained from Gibco Invitrogen (Paisley, UK), with Costar 96-well plates obtained from Corning Incorporate (Corning NY, USA). Bovine serum albumin (BSA), 3-(4, 5-dimethylthiazol-2-yl)-2, 5-diphenyltetrazolium bromide (MTT) and 3,3′,5,5′-Tetramethylbenzidine (TMB) were all obtained from Sigma Chemical Co. (St. Louis MO, USA). Propidium iodide (PI) was procured from ThermoFisher Scientific Inc. (Waltham MA, USA), The Annexin V/PI apoptosis detection kit was from Biovision (Milpitas CA, USA) and DCFDA (2′, 7′-dichlorofluorescein diacetate) cellular reactive oxygen species (ROS) detection assay kit

was obtained from Abcam (Cambridge, UK). Radioimmunoprecipitation assay (RIPA) lysis buffer was purchased from Roche Life Sciences (0724843100, Switzerland), protease inhibitors from Calbiochem (Darmstadt, Germany) and polyvinylidene difluoride (PVDF) membrane from Millipore (Darmstadt, Germany). Antibodies to caspase-8 (catalogue # PA1-29159) was from ThermoScientific (Rockford, USA), caspase-9 (# SC-133109) from Santa Cruz (Dallas TX, USA), caspase-3 (# 9668S) and Poly (ADP-ribose) polymerase (PARP-1) (# 9542S) were from Cell Signaling Technology (Danvers MA, USA), cytochrome c (# 2119-1) was from Epitomics (Burlingame CA, USA). The anti-human β-actin antibody was procured from Santa Cruz. Chemiluminescence, Clarity Western ECL substrate kit was obtained from Bio-Rad (Hercules CA, USA) and X-ray film was obtained from Kodak. AFP and mouse anti-human AFP monoclonal antibody (MBS311557) were purchased from MyBioSource Inc. (San Diego CA, USA). Fucose-binding lectins LCA and AOL were obtained from Vector labs, USA and TCI Japan respectively. All other reagents used were of analytical grade.

2.1 Patient serum samples

Peripheral blood samples from HCC patients and healthy volunteers were collected with prior ethical committee approval (reference number - KCTRI-EC-01/2017) from the Karnatak Cancer Therapy and Research Institute, Padmashree Dr. R. B. Patil Hospital, Hubli, Karnataka, India.

2.2 Purification of ANL

Purification of ANL from mycelial mat was carried out as previously described using mucin-Sepharose 4B affinity column chromatography (11). Conjugation of ANL to FITC was performed as described by Goldman, 1968 (14). Briefly, ANL (5 µg/mL) was incubated with

FITC at 25 μg/mL of protein in carbonate buffer (0.05M, pH 9.5) with gentle stirring overnight at 4°C. Excess, unbound FITC was removed by extensive dialysis against phosphate-buffered saline (PBS) pH 7.3, and FITC-conjugated ANL was stored at 4°C until further use.

2.3 Cell culture

The human hepatocellular carcinoma HepG2 (ATCC# HB-8065) and colon epithelial cancer HT-29 (ATCC# HTB-38) cell lines were procured from American Type Culture Collection (ATCC; Rockville MD, USA) and maintained in DMEM supplemented with 10% v/v foetal calf serum (FCS), 1 mM glutamine, 1 mM sodium pyruvate, 100 mg/mL streptomycin and 100 U/mL penicillin, at 37°C in 5% CO_2 and 95% humidified air.

2.4 Binding studies of ANL with cancer cells as assessed by flow cytometry

HepG2 and HT-29 cells (0.2 x 10^6) were each incubated with 3% w/v BSA to block non-specific sites (1h) and then stained with FITC-conjugated ANL (2 μg) for 1h at 4°C. Carbohydrate-mediated binding was analyzed by pre-incubating the FITC-ANL with 100 g/mL of competing L-fucose and porcine mucin for 1h at 37°C before cell staining. Data was acquired for 10,000 events using a FC500 flow cytometer (Beckman Coulter), and were analyzed using CXPAnalysis software version 2.2. Unstained cells processed similarly were used as a negative control.

2.5 Lectin histochemistry using biotinylated ANL

Biotin-conjugated ANL (5 μg/mL), prepared as described by Boland, 1991 (15), was used for lectin histochemistry. Human CRC (primary and metastatic) and normal tissue samples (patients

without organic disease) were obtained from S. L. Raheja Hospital (Mumbai, India) with prior ethical committee approval (IRB No.08/2009). Tissues obtained during surgery or following colonoscopic polypectomy, were fixed in buffered formalin and embedded in paraffin wax for routine pathological examination. For lectin histochemistry, 5 μm sections were prepared after the pathological diagnosis was confirmed: Normal, primary and metastatic cancer tissues sections were used. Binding of biotinylated-ANL was evaluated using Streptavidin-horseradish peroxidase DAB system through optical analysis.

2.6 Assessment of ANL on HepG2 and HT-29 cell viability

To study the cytotoxic/anti-proliferative action of ANL on cancer cells, HepG2 and HT-29 cells were seeded in 96-well plates (density 5×10^4 cells/mL) and grown in complete medium for 24h prior to lectin treatment. Medium was removed and replaced with serum-free DMEM for 48h, then treated with ANL at different concentrations (0.15–20 μg/mL) and maintained in humidified atmosphere (37°C, 5% CO_2) for 24h and 48h. At each time point, 50 μL of MTT (5 mg/mL) was added to each well followed by lysis with 100 μL dimethyl sulfoxide (DMSO). To observe effects of competing glycan, ANL (5 μg/mL) was pre-incubated for 1h with 100 μg/mL of L-fucose or mucin from porcine, before addition to cells, and processed at 24h and 48h as mentioned above. Cell viability was quantified by measuring absorbance at 570 nm using a micro-plate reading spectrophotometer. Percentage viable cell number was calculated, by comparing to untreated controls, considered as 100%.

2.7 Activity of ANL on the cell cycle

To evaluate the effect of ANL on cell cycle regulation, HepG2 cells were treated with or without ANL (1.25 µg/mL) for 24h and 48h. Cells were harvested after gentle trypsinization (30 seconds), washed with sterile PBS and fixed in ice-cold 70% v/v ethanol for 30 min, at 4 °C. Following fixation, cells were washed again in PBS and treated with 50 µL DNase-free Ribonuclease A (5 mg/mL in PBS) for 10 min at room temperature. Cells were then stained with 450 µL PI (50 µ/mL PBS) for 2h in the dark. DNA content was analyzed on FL-2 channel of flow cytometer (Beckman Coulter FC500). Data was analyzed using Cell Quest Pro software (BD Biosciences) for distribution of cells in different phases of the cell cycle.

2.8 Assessment of ANL-mediated cellular apoptosis

To determine the effect and signaling mechanism involved in ANL-mediated cytotoxicity of HepG2 and HT-29 cancer cells, FITC-annexin V staining was used to monitor for phosphatidylserine externalization, a characteristic feature of cellular apoptosis. Cells treated with ANL (as described above) were harvested by gentle trypsinization and resuspended in binding buffer from the Biovision Annexin V/PI kit. Briefly, cells were incubated with 5 µL FITC-Annexin V and 5 µL PI for 15 min at 37°C in the dark, before analysis by flow cytometry. The percentage of cells positive for Annexin V, PI alone and both Annexin V and PI were calculated by dot plot analysis using CXP analysis software version 2.2, Beckman Couter).

2.9 Determination of ANL-activated release of reactive oxygen species (ROS)

To determine the release of intracellular ROS in HepG2 cells following lectin treatment, a cellular ROS detection assay kit was used utilizing the cell permeant fluorogenic dye 2′, 7′-dichlorofluorescin diacetate (DCFDA). which is deacetylated by intracellular esterases to a

nonfluorescent compound, and in the presence of ROS is oxidized to a highly fluorescent compound 2′, 7′-dichlorofluorescein (DCF). Cells (2 × 10^4 cells/treatment) in incomplete or serum free DMEM (plain DMEM) were incubated with DCFDA (50 ng/mL) for 30 min and then treated with ANL (IC_{50}) for 4h in dark, at 37°C. Fluorescence data was acquired using a Tecan Infinite 200 microplate reader (Tecan; Männedorf, Switzerland) with excitation and emission wavelengths of 495 nm and 529 nm, respectively. Cells treated with ROS-inducing tert-butyl hydroperoxide (tBHP, at 50µM and PBS alone served as positive and negative controls, respectively.

2.10 Determination of ANL-induced change in mitochondrial membrane potential (MMP)

HepG2 cells (0.2 × 10^6 cells/mL) were grown on cover slips in complete DMEM medium for 48h and were treated with ANL 1.25µg/ml (IC_{50}) for 48h in serum-free media. Cells were washed with PBS and stained with a cell permeant dye that accumulates within active mitochondria, tetramethyl-rhodamine methyl ester (TMRM). ANL-induced changes in MMP of the treated cells was observed using a Motic BA410 fluorescence microscope (400X magnification), photographed, and images compared to untreated control.

2.11 Immunoblot analysis to delineate ANL-induced signaling pathways

To delineate the signaling mechanism involved in ANL-induced apoptosis, HepG2 cells were treated with ANL (1.25 µg/mL) for different time intervals, up to 48h. Following treatment, cells were lysed in RIPA buffer, 2 mM EDTA, protease inhibitor cocktail; and total protein 60µg per each well was electrophoresed on SDS–polyacrylamide gels (12%) and then blotted to PVDF membrane. Membranes were blocked with 5% w/v BSA in PBS, and then probed with primary

antibodies to caspase-8, -9, acaspase-3, cytochrome c and PARP-1 for 1h at room temperature, followed by incubation of species-specific HRP-conjugated secondary antibodies for 1h. Blots were washed and processed using the Clarity Western ECL substrate kit, with chemiluminescence signals recorded on X-ray film. Antibody detection of β-actin was used as a loading control to normalize changes in levels of other proteins detected.

2.12 Lectin sandwich ELISA using ANL and anti-AFP detection antibody

To evaluate clinical diagnostic potential of ANL in detection of tumour-associated, fucosylated serum proteins, 96-well high-binding, enzyme-linked immunosorbent assay (ELISA) plates were coated with ANL (5 μg/well) followed by overnight incubation at 4°C, the plate was washed thrice with 0.05% v/v Tween 20 in PBS (PBST) for 3 min each. Unbound sites were blocked with 3% w/v BSA in PBS, at 37°C for 1h. After washing, a calibration curve using different concentrations of AFP (5, 10, 20, 40, 80, 100, 200 and 400 ng/ml) dissolved in 50 μL PBS and 50 μl normal serum from healthy human volunteers was generated applied to each well of the microtiter plate, or a 1:10 dilution of serum samples from HCC patients and normal healthy volunteers (two of each) were added. After incubation at 37°C for 1h, the plate was washed, and 50 μL of anti-human AFP antibody (1:1000 dilution) in 1% w/v BSA in PBST were added. After incubation at 37°C for 1h, the plates were washed and then species-specific HRP-conjugated secondary antibody against AFP-antibody was added. After incubation at 37°C for 1h, the plate was washed and then 100 μL of freshly prepared TMB substrate was added. After incubation for 15 min in dark, the enzymatic reaction was stopped by adding 25μL of 5N sulphuric acid and read at optical density (OD) 450 nm. Commercially available fucose-binding lectins LCA and AOL were used as positive controls. To validate carbohydrate-dependent interaction of ANL,

AOL and LCA to AFP, each lectin was pre-incubated with competing fucose and mucin (100 µg/mL) prior to addition of AFP. All the experiments were performed in duplicate.

2.13 Statistical analysis

Results were expressed as mean ± SD. Statistical comparisons were performed using the Student's t-test in order to determine statistical significance. Microsoft Excel was used to perform statistical analysis.

3. Results

3.1 ANL and AOL strongly bind to HepG2 and HT-29 cells

Interaction with HepG2 and HT-29 cells was determined by staining cells with FITC-conjugated lectins followed by flow cytometric analysis. A total of 93.49% HepG2 cells showed positive staining for ANL and 90.32% for AOL (with mean fluorescence intensity (MFI) of 183 and 153 compared to unstained cells; MFI of 3.12 for ANL and 2.4 for AOL, respectively); see **Figure 1**. Carbohydrate-dependent interaction of both ANL and AOL to HepG2 cells was determined using competing sugars/glycoconjugates, which resulted in significant reduction in cell-surface binding of each lectin. For HepG2 cells stained with FITC-ANL, MFI decreased to 24.8 and 133 in presence of L-fucose and mucin, respectively; similar decreases were also seen in FITC-AOL interaction with L-fucose and mucin pre-treatment, with MFI of 35 and 85 respectively (**Figure 1**). For both lectins, L-fucose was seen to be the most effective inhibitor.

For HT-29 cells, a total of 75.63% stained positive for FITC-conjugated ANL and 63.5% for FITC-AOL (with MFI of 90.5 and 76.6 for ANL and AOL, compared to unstained cells with

MFI of 30 and 32 respectively); (**Figure 2)**. MFI decreased to 45.2 and 38.2 for HT-29 cells stained with ANL and AOL when pre-incubated with mucin (**Figure 2**)

3.2 ANL and AOL inhibit the growth of HepG2 and HT-29 cells

Fucose-binding lectins ANL and AOL both significantly inhibited growth of HepG2 and HT-29 cells in a dose- and time-dependent manner (**Figure 3**). Maximum reduction in cell viability was seen at 20 µg/mL lectin over 48h, with ANL and AOL inhibiting cellular growth of HepG2 cells by 89.5 ± 0.02 % and 85.6 ± 0.05 %, respectively). Similarly, both ANL and AOL inhibited growth of HT-29 cells at 48h by 85.2 ± 0.06% and 80.6 ± 0.04%, respectively. In presence of competing mucin glycoprotein, the ANL-and AOL-induced growth inhibitory effect on HepG2 cells (at 5 µg/mL) was effectively blocked by 79.65 ± 0.09% and 82.97 ±0.03% respectively; (**Figure 3**). IC_{50} value of ANL for HepG2 cells was found to be 1.25µg/ml at 48 h. Likewise, ANL and AOL-induced inhibition of growth observed for HT-29 cells was also effectively blocked by 74.65±0.05% and 79.97±0.01% respectively in presence of mucin (**Figure 3**). IC_{50} value of ANL for HT-29 cells was found to be 2.5µg/ml at 48 h. These results show that ANL and AOL inhibit the growth of liver and colon cancer cells by interaction with cell-surface glycans.

3.3 ANL increases hypodiploidy and decreases the G_0/G_1 population in HepG2 cells

HepG2 cells, treated with ANL IC_{50} (1.25 µg/mL) for 24h and 48h, were stained with PI and subjected to flow cytometry, so as to determine the distribution of cells at different phases of the cell cycle and the percentage of cells undergoing apoptosis. Treatment of HepG2 cells with ANL for 24h increased the hypodiploid cell population by 8.4% compared to 1.3% in the untreated

control cell population; at 48h, this rose to 16.5% compared to 2.8%, respectively (**Figure 4**). Concomitant decreases were observed in the G_0/G_1 and G_2/M cell populations at 24h and 48h time points following ANL treatment, compared to untreated controls (**Figure 4** and **Table 1**).

3.4 ANL induces apoptosis in HepG2 and HT-29 cells

To assess whether the observed growth inhibitory effect of ANL on HepG2 and HT-29 cells was due to induction of apoptosis, cells were analysed for phosphatidylserine externalization by staining with Annexin V/PI. ANL with IC_{50} of 1.25 µg/ml, 2.5 µg/ml for HepG2 and HT-29 respectively treated cells showed 12.1% (for HepG2) and 24.6% (HT-29) of the cell population were in the early phase of apoptosis at 24h, and 24.6% (HepG2) and 28.8% (HT-29) at 48h, compared to untreated control cells (0.2% and 7.5% for HepG2 and 7.9% and 12.1% for HT-29, at 24h and 48h respectively); Furthermore, ANL treatment also increased numbers of cells in the late apoptotic phase, with HepG2 cells by 2.4% and 8.0% (at 24h and 48h) compared to untreated controls (0.1% and 6.3%); and similarly, for HT-29 3.6% and 5.1% (at 24h and 48h) compared to control (1.9% and 2.1%, respectively); see **Figure 5** and **Table 2**. Significant increases in early and late apoptotic population supports induction of apoptosis in both HepG2 and HT-29 cells by ANL.

3.5 ANL increases cellular ROS levels and induces apoptosis involving intrinsic apoptotic pathway in HepG2 cells

An increase in level of ROS is a sign of apoptosis induction through oxidative stress or DNA damage. Treatment of HepG2 cells with ANL for 4h resulted in increased generation of ROS by 22.67 ± 0.06 (mean ± SD) and 28.67± 0.01 -fold, at doses of 2 and 4 µg/ml lectin, respectively

indicating elevated levels of cellular oxidative stress (**Figure 6A**). Loss of mitochondrial membrane potential (MMP) followed by the release of apoptotic factors, release of cytochrome c and loss of oxidative phosphorylation indicate an induction of apoptosis. HepG2 cells treated with ANL (1.25 μg/mL (IC_{50}), for 48h) showed characteristic depolarization of mitochondrial membrane as revealed by microscopy, with significant decrease in fluorescence observed in ANL-treated cells indicating loss of MMP, compared to untreated control cells which showed intact mitochondria with strong bright red-orange fluorescence signal (**Figure 6B**).

To delineate the mechanism of ANL-induced apoptosis in HepG2 cells, effects of ANL on activation of initiator caspases-8, - 9 and effector caspase-3 were measured. A time-dependent increase in active caspase-9, active caspase-3 was observed (**Figure 6C**). There was also time-dependent increase in levels of cytochrome c by ANL. No detection of caspase-8 was seen. Taken together, these results imply that ANL induces an increase in cellular ROS, loss of MMP and induction of cellular apoptosis involving the intrinsic apoptotic pathway in HepG2 cells. ANL also induced the increase in expression of active caspase-3 in HT-29 cells (data not presented as supplementary data) indicating apoptotic effects on these cells.

3.6 ANL shows differential binding to human colon cancer and normal tissues

In order to test the diagnostic potential of ANL, lectin histochemistry was performed with normal colonic tissue, and primary and metastatic human colon cancer tissues using biotinylated ANL. ANL showed strong binding to both primary and metastatic colon cancerous tissues and no binding to normal colon tissues; see **Figure 7**. The differential binding of ANL to normal and primary, metastatic cancer tissues reveals the potential of ANL as possible diagnostic tool.

3.7 Sandwich ELISA using ANL and anti-AFP antibody

In order to further evaluate the diagnostic potential of ANL, serum samples collected from normal and HCC patients were tested by using a lectin sandwich ELISA to capture and then quantify AFP in serum, using ANL and an anti-human AFP antibody (see **Figure 8)**. A dose-dependent linear increase in absorbance was observed for standard AFP dissolved either in PBS (**Figure 8.A**) or in serum (10%) from healthy volunteers (**Figure 8.B**) using ANL as the capture lectin. Similar results were obtained using two other fucose-binding lectins, LCA and AOL coated to the ELISA plates. Very low levels of AFP were captured by all three fucose-binding lectins in the normal serum samples (as indicated by low absorbance values), whereas HCC patients samples showed significantly higher levels of AFP in serum; see **Figure 8. A-B**. Carbohydrate-dependent binding of ANL, LCA and AOL to AFP was validated by pre-incubation with competing L-fucose or mucin (at 10μg/mL) prior to addition of APF in the assay. There was a significant inhibition in lectin binding to AFP by 99% and 95% for ANL, 88.5% and 82% for LCA, and by 97% and 91% for AOL (**Figure 8**. **C-E**) when pre-incubated with L-fucose and mucin respectively; These encouraging results indicate that the lectin-antibody sandwich ELISA using ANL is effective in detecting elevated levels of fucosylated-AFP in patient cancer serum samples.

5. Discussion

Here we studied the L-fucose-specific lectin from *Aspergillus niger,* ANL, to evaluate its anti-cancer properties and diagnostic potential for liver and gastrointestinal cancers. The study

demonstrates that ANL exerts remarkable growth inhibitory effects on human hepatocellular carcinoma cells and colon cancer epithelial cancer cells in a dose- and time-dependent manner. The observed growth inhibitory effect of ANL is due to induction of apoptosis through the intrinsic pathway, thereby supporting its anti-cancer potential. ANL differentially binds to normal and cancerous tissues, and can be utilized to provide sensitive detection of AFP, comparable to LCA, in normal and HCC serum samples, thus demonstrating its diagnostic potential.

Lectins in general, and in particular fucose-specific lectins, have been shown to play an important role in identifying aberrant glycosylation that occurs in pathological conditions, such as in inflammation and cancer, and hence are studied for potential clinical applications (5). Lectins, from both plants and fungi, are known to induce proliferative/anti-proliferative effects *in vitro* upon binding to many types of human cancer cells (16). As previously reported, ANL strongly binding to PANC-1 cells here we report ANL strongly binds to HepG2 and HT-29 cells. The surface binding and population growth inhibitory effect of ANL on HepG2 and HT-29 cells which can be effectively blocked by L-fucose and mucin suggesting involvement of cell-surface glycans in binding and consequent inhibition of cell proliferation. Induction of apoptosis by ANL was demonstrated by increase in the hypodiploid cell population, elevated annexin-V positivity, followed by immunoblot analysis identifying key caspases regulating cell death (17), particularly elevation of levels of apoptosis initiator caspase 9 and activation of caspase 3. Lectins in general are known to induce cell cycle arrest at either G_0/G_1, S, or G_2/M phases, or in combination, to induce apoptosis. A noted example is the mitogenic fungal lectin RBL, from *Rhizoctonia bataticola,* which arrests cell growth of the human metastatic colon cancer cell-line SW620, increasing the number sub-G_1 hypodiploid cells within the population in a time-dependent

manner – a typical marker of apoptosis (18, 19). RBL also induces apoptosis in SW620 cells by production of excess ROS which leads to nuclear degradation (18). In the present study, ANL shows similar action, increasing the hypodiploid population in HepG2 cells and concomitant reduction in G_0/G_1, S and G_2/M phases, suggesting induction of apoptosis at particular phases of the cell cycle. Annexin-V-FITC and PI double-staining of ANL-treated HepG2 and HT-29 cells showed increases in the early and late apoptotic cell populations in a time dependent manner. Other fucose-binding lectins affect many physiological activities like induction of autophagy, apoptosis, or necrosis, in different cell-lines (20). *Dicentrarchus labrax* fucose-binding lectin (DIFBL) similarly induces apoptosis in liver cancer cell-lines Hep3B and BEL-7404, in A549 lung cancer cells, and in the colorectal carcinoma cell-line SW480 (20). In comparison with these lectins, ANL also induced apoptosis indicating its high potency. Recently we have reported a similar effect with core fucose specific lectin CSL another mitogenic lectin form *Cephalosporium curvulum* a pathogenic fungus knowing for causing mycotic keratitis possibly through intrinsic apoptotic pathway in PANC-1 and HepG2 cells (10).

Increased level of ROS plays an important role in induction of apoptosis through oxidative stress or DNA damage (21), with ROS released by, or targeting, mitochondria, promoting cytochrome c release that triggers caspase activation (22). Currently, popular anti-cancer drugs like adriamycin, epirubicin, and daunomycin being used to treat many types of cancer are known to induce apoptosis and exert anti-tumour effects through the generation of ROS, leading to loss in MMP (23). We showed here that ANL can increase ROS production and decrease MMP in HepG2 cells, which likely indicates activation of the intrinsic apoptotic pathway. Other lectins, well known for their anti-cancer actions, are also reported to induce the intrinsic pathway of apoptosis through the production of ROS leading to change in MMP. The mannose-specific

lectin Concanavalin A (ConA) has been shown to induce caspase-dependent apoptosis in human melanoma A375 cells by increasing cytochrome c levels, with subsequent stimulation of caspase-9 and activation of caspase-3 levels – all indicative of mitochondrial-mediated apoptosis (16). ConA binds to the cell surface membrane and induces autophagy in the hepatoma cell-line ML-1 by preferentially accumulating in mitochondria, subsequently leading to a change in MMP (24). Cell death is an important phenomenon that involves participation of different effector caspases, which can execute either intrinsic or extrinsic pathways (17,25). Signals like ROS and cytochrome c are known apoptotic factors, which within the mitochondria trigger the intrinsic apoptotic pathway via activation of initiator caspase-9 (26). ANL clearly activates caspase-9, and not the extrinsic apoptosis pathway initiator caspase-8, followed by cleavage of executioner caspase-3, suggesting involvement of intrinsic caspase dependent apoptotic pathway.

Fucose-specific lectins have shown to play an important role in identifying aberrant fucosylation in pathological conditions, such as cancer (5). AFP is an important serum glycoprotein which is aberrantly glycosylated and secreted by hepatocellular carcinomas (27-29). Hence AFP is the most reliable widely used tumor marker for the diagnosis of HCC. High serum levels of AFP of more than 20 ng/mL can be directly related to high risk for HCC (30, 31).

A well-known fucose-binding lectin from the Orange peel fungus *Aleuria aurantia* (AAL), recently bioengineered as a monomeric form AAL-S2 with high affinity towards α1–6 fucosylated (core-fucosylated) glycans (32), was used to construct a reverse-lectin ELISA method to support identification of aberrantly fucosylated alpha-1 acid glycoprotein in the serum of HCC patients (33). Immuno-histochemical studies revealed its diagnostic potential by differentially binding to normal and metastatic cancerous tissues (34). We have recently shown that a lectin sandwich ELISA using CSL (10), a core fucose-specific lectin from *Cephalosporium*

curvulum, is effective also in detecting aberrantly fucosylated AFP in the serum of cancer patients when compared to another fucose-binding lectin from *Lens culinaris,* LCA (10). As fucose-specific lectins are known for their role in identifying aberrant fucosylation of glycoproteins in cancer, ANL was studied here to quantify the AFP levels in the serum samples of normal and HCC patients. Our lectin-ELISA results show clearly that ANL can identify AFP as low as 5 ng demonstrating its high sensitivity, comparable with LCA, a fucose-specific lectin currently used for detecting AFP levels in HCC diagnosis (35).

In conclusion, fucose-specific lectin ANL inhibits cell proliferation and induces apoptosis, in gastrointestinal HepG2 and HT-29 cancer cells. This activity could be effectively blocked by competing L-fucose and fucosylated glycans on mucin. ANL induces cellular apoptosis by production of ROS, change in MMP involving activation of caspases-9 and caspase-3 suggesting involvement of intrinsic apoptotic pathway. ANL has diagnostic potential as revealed by our data using an ANL-anti AFP antibody sandwich ELISA and ANL-histochemistry using colon cancer tissue samples. In conclusion, the present study indicates the potential of ANL in hepatic and colon cancer research both for its anti-cancer effect as well as for diagnostic purposes.

Author contributions: All authors contributed to the study. Performed experiments and first draft of the manuscript (Narasimhappagari Jagadeesh); flow cytometry (Narasimhappagari Jagadeesh & Shivakumar Belur); study conception, design, and laboratory facilities (Shashikala R. Inamdar), intellectual support, and final manuscript (Barry J. Campbell & Shashikala R. Inamdar). All authors read and approved the final manuscript.

Disclosure of interest: Authors declare no conflict of interest.

References

1. Marth JD. Glycosylation changes in ontogeny and cell activation. *Glycobiology*. 1999:515-36.
2. Fuster MM, Esko JD. The sweet and sour of cancer: glycans as novel therapeutic targets. *Nat Rev Cancer*. 2005 (7):526-42.
3. Hutchinson WL, Du MQ, Johnson PJ, Williams R. Fucosyltransferases: differential plasma and tissue alterations in hepatocellular carcinoma and cirrhosis. *Hepatology.* 1991 :683-8.
4. Miyoshi E, Moriwaki K, Terao N, Tan CC, Terao M, Nakagawa T, Matsumoto H, Shinzaki S, Kamada Y. Fucosylation is a promising target for cancer diagnosis and therapy. *Biomolecules*. 2012:34-45.
5. Ohtsubo K, Marth JD. Glycosylation in cellular mechanisms of health and disease. *Cell*. 2006,855-67.
6. Hollingsworth MA, Swanson BJ. Mucins in cancer: protection and control of the cell surface. *Nat Rev Cancer*. 2004:45-60.
7. Moriwaki K, Miyoshi E. Fucosylation and gastrointestinal cancer. *World J Hepatol.* 2010 :151.
8. Pekelharing JM, Vissers P, Peters HA, Leijnse B. Lectin-enzyme immunoassay of transferrin sialovariants using immobilized antitransferrin and enzyme-labeled galactose-binding lectin from Ricinus communis. *Anal Biochem.* 1987 :320-6.

9. Kinoshita N, Ohno M, Nishiura T, Fujii S, Nishikawa A, Kawakami Y, Uozumi N, Taniguchi N. Glycosylation at the Fab portion of myeloma immunoglobulin G and increased fucosylated biantennary sugar chains: structural analysis by high-performance liquid chromatography and antibody-lectin enzyme immunoassay using Lens culinaris agglutinin. *Cancer Res*. 1991 5888-92.
10. Belur S, Jagadeesh N, Swamy BM, Inamdar SR. A core fucose specific lectin from Cephalosporium curvulum induces cellular apoptosis in hepatocellular and pancreatic cancer cells and effective in detecting AFP. *Glycoconj J*. 2020 :1-0.
11. Jagadeesh N, Belur S, Hegde P, Kamalanathan AS, Swamy BM, Inamdar SR. An L-fucose specific lectin from Aspergillus niger isolated from mycotic keratitis patient and its interaction with human pancreatic adenocarcinoma PANC-1 cells. *Int J Biol Macromol.* 2019 :487-97.
12. Kaur S, Kumar S, Momi N, Sasson AR, Batra SK. Mucins in pancreatic cancer and its microenvironment. *Nat Rev Gastroenterol Hepatol.* 2013 :607.
13. Gao HF, Wang QY, Zhang K, Chen LY, Cheng CS, Chen H, Meng ZQ, Zhou SM, Chen Z. Overexpressed N-fucosylation on the cell surface driven by FUT3, 5, and 6 promotes cell motilities in metastatic pancreatic cancer cell lines. *Biochem Biophys Res Commun*. 2019 :482-9.
14. Goldman M. Fluorescent antibody methods.
15. Boland CR, Chen YF, Rinderle SJ, Resau JH, Luk GD, Lynch HT, Goldstein IJ. Use of the lectin from Amaranthus caudatus as a histochemical probe of proliferating colonic epithelial cells. *Cancer research*. 1991 :657-65.

16. Yau T, Dan X, Ng CC, Ng TB. Lectins with potential for anti-cancer therapy. *Molecules*. 2015 :3791-810.

17. Grütter MG. Caspases: key players in programmed cell death. *Curr Opin Struct Biol* 2000 :649-55.

18. Hegde P, Rajakumar SB, Swamy BM, Inamdar SR. A mitogenic lectin from Rhizoctonia bataticola arrests growth, inhibits metastasis, and induces apoptosis in human colon epithelial cancer cells. *J Cell Biochem.*2018 :5632-45.

19. Riccardi C, Nicoletti I. Analysis of apoptosis by propidium iodide staining and flow cytometry. *Nature protocols*. 2006 :1458-61.

20. Wu L, Yang X, Duan X, Cui L, Li G. Exogenous expression of marine lectins DlFBL and SpRBL induces cancer cell apoptosis possibly through PRMT5-E2F-1 pathway. *Sci Rep*. 2014 :4505.

21. Finkel T. Oxidant signals and oxidative stress. C*urr Opin Cell Biol*. 2003 :247-54.

22. Simon HU, Haj-Yehia A, Levi-Schaffer F. Role of reactive oxygen species (ROS) in apoptosis induction. *Apoptosis*. 2000 :415-8.

23. Xia Z, Lundgren B, Bergstrand A, DePierre JW, Nässberger L. Changes in the generation of reactive oxygen species and in mitochondrial membrane potential during apoptosis induced by the antidepressants imipramine, clomipramine, and citalopram and the effects on these changes by Bcl-2 and Bcl-XL. *Biochem Pharmacol.* 1999 :1199-208.

24. Chang CP, Yang MC, Liu HS, Lin YS, Lei HY. Concanavalin A induces autophagy in hepatoma cells and has a therapeutic effect in a murine in situ hepatoma model. *Hepatology*. 2007 :286-96.

25. Elmore S. Apoptosis: a review of programmed cell death. *J Toxicol Pathol.* 2007 :495-516.

26. Wang X. The expanding role of mitochondria in apoptosis. *Genes & development.* 2001 :2922-33.

27. Huang Y, Wu H, Xue R, Liu T, Dong L, Yao J, Zhang Y, Shen X. Identification of N-glycosylation in hepatocellular carcinoma patients' serum with a comparative proteomic approach. *PLoS One*. 2013):e77161.

28. Mehta A. Glycosylation and hepatacellular carcinoma. Encyclopedia of Genetics, Genomics, Proteomics and Bioinformatics. 2004 : 15.

29. Ajdukiewicz AB, Kelleher PC, Krawitt EL, Walters CJ, Mason PB, Koff RS, Bélanger L. α-Fetoprotein glycosylation is abnormal in some hepatocellular carcinomas, including white patients with a normal α-fetoprotein concentration. *Cancer Lett*. 1993 :43-50.

30. Alpert E, Hershberg R, Schur PH, Isselbacher KJ. α-Fetoprotein in human hepatoma: improved detection in serum, and quantitative studies using a new sensitive technique. *Gastroenterology*. 1971 :137-43.

31. Okuda K, Kotoda K, Obata H, Hayashi N, Hisamitsu T, Tamiya M, Kubo Y, Yakushiji F, Nagata E, Jinnouchi S, Shimokawa Y. Clinical observations during a relatively early stage of hepatocellular carcinoma, with special reference to serum α-fetoprotein levels. *Gastroenterology*. 1975 :226-34.

32. Guo YL, Zhang YL, Zhu JQ. Prognostic value of serum α‐fetoprotein in ovarian yolk sac tumors: A systematic review and meta‐analysis. Molecular and clinical oncology. 2015 :125-32.

33. Åström E, Stål P, Zenlander R, Edenvik P, Alexandersson C, Haglund M, Ryden I, Påhlsson P. Reverse lectin ELISA for detecting fucosylated forms of α1-acid glycoprotein associated with hepatocellular carcinoma. PloS one. 2017 :e0173897.
34. Olausson J, Åström E, Jonsson BH, Tibell LA, Påhlsson P. Production and characterization of a monomeric form and a single-site form of Aleuria aurantia lectin. Glycobiology. 2011:34-44.
35. Song BC, Suh DJ, Yang SH, Lee HC, Chung YH, Sung KB, Lee YS. Lens culinaris agglutinin-reactive alpha-fetoprotein as a prognostic marker in patients with hepatocellular carcinoma undergoing transcatheter arterial chemoembolization. Journal of clinical gastroenterology. 2002 :398-402.

Table 1: Effect of the fucose-specific *Aspergillus niger* lectin (ANL) on different phases of cell cycle in HepG2 hepatocellular carcinoma cells.

Phase of the cell cycle	Percentage of cells in different phases			
	24h		48h	
	Control	ANL*	Control	ANL*
Hypodiploid	1.3	8.4	2.8	16.5
G_0/G_1	68.2	67.4	72.3	62.1
S	10.4	7.5	8.9	7.5
G_2/M	18.9	13.7	14.8	11.6

***ANL treatment (1.25 µg/mL)**

Table 2: Annexin V-PI staining of *Aspergillus niger* lectin (ANL)-treated HepG2 and HT-29 cells

Phase	HepG2 cells				HT-29 cells			
	24h		48h		24h		48h	
	Control	ANL*	Control	ANL*	Control	ANL**	Control	ANL**
Normal	99.1	83.6	82.4	66.2	88.6	70.3	84.3	65.7
Necrotic	0.6	1.9	3.9	1.2	1.6	0.9	1.5	0.5
Early apoptotic	0.2	12.1	7.5	24.6	7.9	25.2	12.1	28.8
Late apoptotic	0.1	2.4	6.3	8.0	1.9	3.6	2.1	5.1

*ANL treatment (1.25 µg/mL)

** ANL treatment (2.5 µg/mL)

Figure Legends

Figure 1. Fucose-binding lectins ANL and AOL strongly bind to HepG2 cells. Human hepatocellular carcinoma HepG2 cells were incubated with either FITC-conjugated ANL **(A1)** or AOL **(B1)** in absence (red line) or presence of competing sugar (L-fucose; blue line) or glycoconjugate (mucin; pink line). Binding was analysed by flow cytometry; with cells untreated with lectin indicated (black line). The overlays are representative data with X-axis and Y-axis expressed as mean fluorescence intensity (MFI) and cell count, respectively. Panels **A2** (ANL) and **B2** (AOL) represent inhibition of binding (MFI) in presence or absence of competing L-fucose (blue bar) or mucin (pink bar) compared to FITC-conjugated lectin alone. (red bar).

Figure 2. ANL and AOL strongly bind to HT-29 cells. Human colonic adenocarcinoma HT-29 cells were incubated with FITC-labeled ANL **(A1)** or AOL **(B1)** in absence (blue line) or in

presence of competing mucin (pink line). Binding was analyzed by flow cytometry; with cells untreated with lectin indicated (black line). The overlays are representative data with X-axis and Y-axis representing fluorescent intensity and cell count, respectively. Panels **A2** (ANL) and **B2** (AOL) represent inhibition of binding (MFI) in presence or absence of competing mucin (pink bar) compared to FITC-conjugated lectin alone (blue bar).

Figure 3. ANL and AOL inhibit growth of HepG2 and HT-29 cells. Both fucose-binding lectins ANL and AOL decreased cell viability/numbers of HepG2 and HT-29 cells over 24h and 48h, as assessed by MTT assay. Data is expressed as % cell viability compared to untreated controls (100%). Mucin (M), at 100 µg/mL, effectively blocked ANL or AOL lectin (L)-mediated inhibition of growth (at 5 µg/mL). Data expressed as mean ± SD of three independent experiments.

Figure 4. ANL increases hypodiploidy and decreases G_0/G_1 population in HepG2 cells. HepG2 cells were incubated with or without ANL (1.25 µg/mL) for either 24h or 48h. Cells were stained with propidium iodide (PI) and data acquired on the FL3 channel of the flow cytometer. B, C, D, and E represent the hypodiploid (apoptotic), G_0/G_1, S, and G_2/M phases, respectively.

Figure 5. ANL induces apoptosis in HepG2 and HT-29 cells. HepG2 **(A)** and HT29 **(B)** cells were analysed by Annexin V/propidium iodide (PI) staining using flow cytometry. ANL (1.25 µg/mL) induced apoptosis in HepG2 cells **(A.1)** and HT-29 cells **(B.1)**. The X-axis depicts Annexin V positive cells, and the Y-axis depicts PI-positive cells. A1, A2, A3 and A4 quadrants represent the necrotic, late apoptotic, normal and early apoptotic cell populations respectively,

with numbers indicating the percentage number of viable, early apoptotic, late apoptotic, and necrotic cells that are present in the respective quadrants. Percentage of the cell populations in different areas are summarised in **(A.2)** and **(B.2)**.

Figure 6. ANL induces oxidative stress, alters mitochondrial membrane potential and induces apoptosis in HepG2 cells. (A) Intracellular production of ROS was measured using a cell permeant fluorogenic dye 2′, 7′- dichlorofluorescin diacetate (DCFDA) and fluorescence was measured by microplate reader. **(B)** Mitochondrial membrane potential (MMP) was measured using tetramethyl-rhodamine methyl ester (TMRM) and fluorescence microscopy. TMRM accumulates within active mitochondria of control cells (left hand panel), with ANL-inducing depolarization of mitochondrial membrane as indicated by a decrease in fluorescence (right hand panel). **(C)** Immunoblot analysis of activation of intrinsic apoptotic pathway in HepG2 cells treated with ANL (IC_{50}) over 48h, indicating increased levels of caspase-3 and -9, cytochrome c and PARP-1. β-actin was used as loading control.

Figure 7. ANL shows differential binding to human colon cancer and normal tissues

Differential binding of ANL to normal and cancerous human colon tissues: ANL shows no binding to normal human colon tissues **(A)** but strong binding to primary cancer **(B)** and metastatic colon **(C)** tissues. Representative images are presented. All the images were obtained with 400X magnification. “Arrows” point to ANL binding to apical surface of the secretory gland epithelia.

Figure 8. Sandwich ELISA using ANL and anti-AFP antibody: AFP was added in varying concentrations dissolved in PBS **(A)** dissolved in normal serum **(B)** for the standard calibration curve, and in another set the normal and HCC patient serum samples diluted 1:50 in PBS. Bound AFP antibodies were detected using HRP-conjugated secondary antibody. Absorbance was read at 450 nm. Competitive inhibition of ANL **(C)**, LCA **(D)** and AOL **(E)** within the ELISA by competing sugar L-fucose or mucin. Both L-fucose and mucin reduced the binding of lectins to AFP (as determined by significant reduction in absorbance).

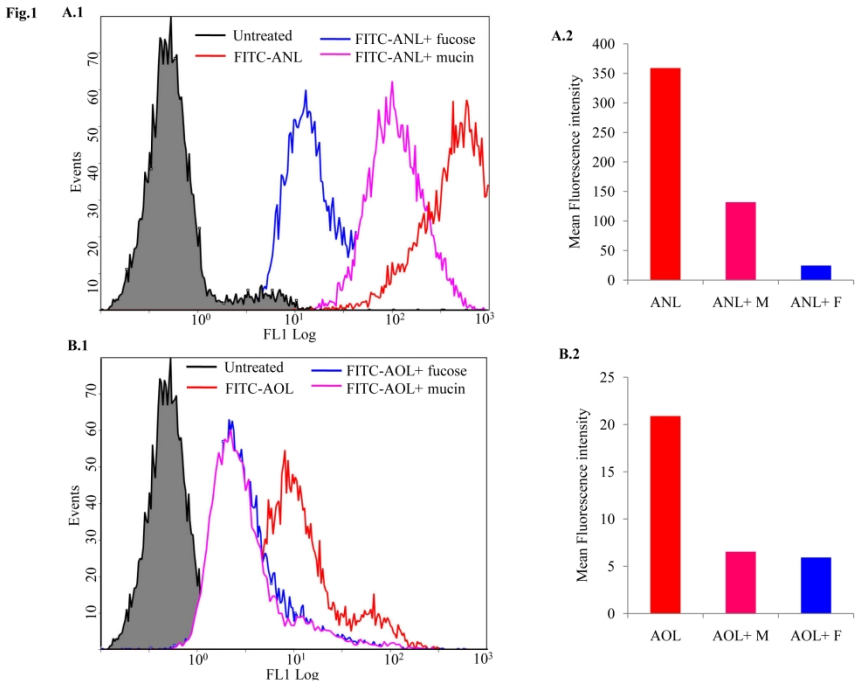

Figure 1. Fucose-binding lectins ANL and AOL strongly bind to HepG2 cells. Human hepatocellular carcinoma HepG2 cells were incubated with either FITC-conjugated ANL (A1) or AOL (B1) in absence (red line) or presence of competing sugar (L-fucose; blue line) or glycoconjugate (mucin; pink line). Binding was analysed by flow cytometry; with cells untreated with lectin indicated (black line). The overlays are representative data with X-axis and Y-axis expressed as mean fluorescence intensity (MFI) and cell count, respectively. Panels A2 (ANL) and B2 (AOL) represent inhibition of binding (MFI) in presence or absence of competing L-fucose (blue bar) or mucin (pink bar) compared to FITC-conjugated lectin alone. (red bar).

279x215mm (300 x 300 DPI)

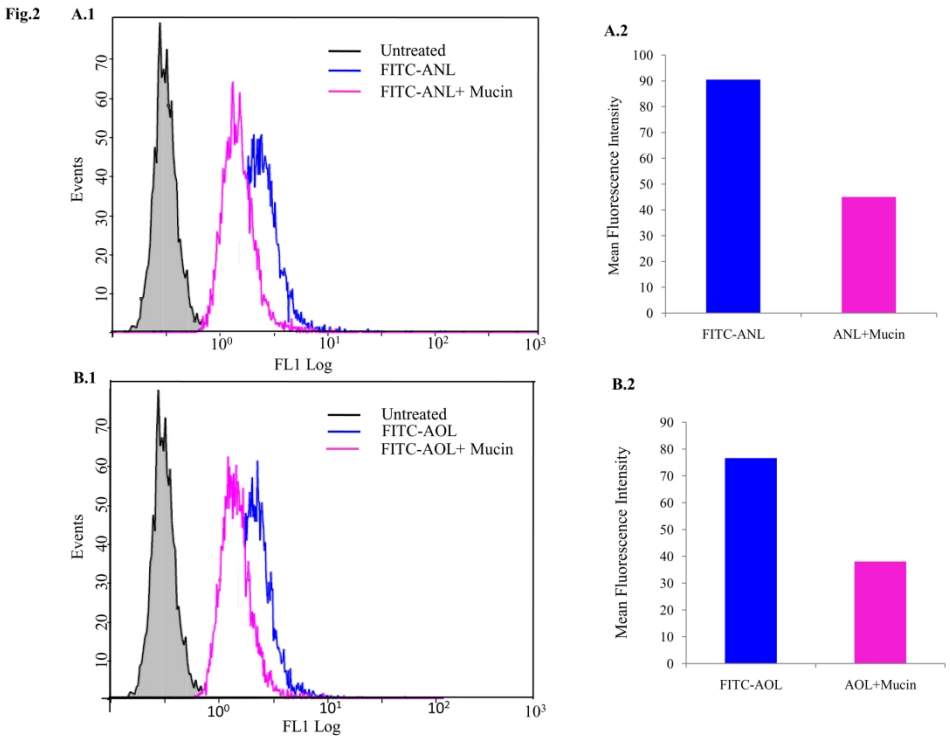

Figure 2. ANL and AOL strongly bind to HT-29 cells. Human colonic adenocarcinoma HT-29 cells were incubated with FITC-labeled ANL (A1) or AOL (B1) in absence (blue line) or in presence of competing mucin (pink line). Binding was analyzed by flow cytometry; with cells untreated with lectin indicated (black line). The overlays are representative data with X-axis and Y-axis representing fluorescent intensity and cell count, respectively. Panels A2 (ANL) and B2 (AOL) represent inhibition of binding (MFI) in presence or absence of competing mucin (pink bar) compared to FITC-conjugated lectin alone (blue bar).

254x190mm (300 x 300 DPI)

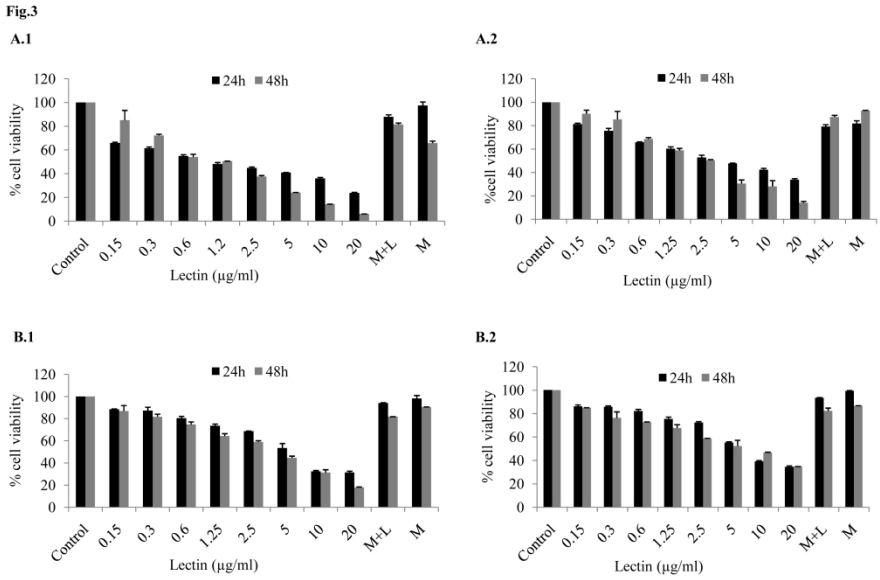

Figure 3. ANL and AOL inhibit growth of HepG2 and HT-29 cells. Both fucose-binding lectins ANL and AOL decreased cell viability/numbers of HepG2 and HT-29 cells over 24h and 48h, as assessed by MTT assay. Data is expressed as % cell viability compared to untreated controls (100%). Mucin (M), at 100 µg/mL, effectively blocked ANL or AOL lectin (L)-mediated inhibition of growth (at 5 µg/mL). Data expressed as mean ± SD of three independent experiments.

279x215mm (300 x 300 DPI)

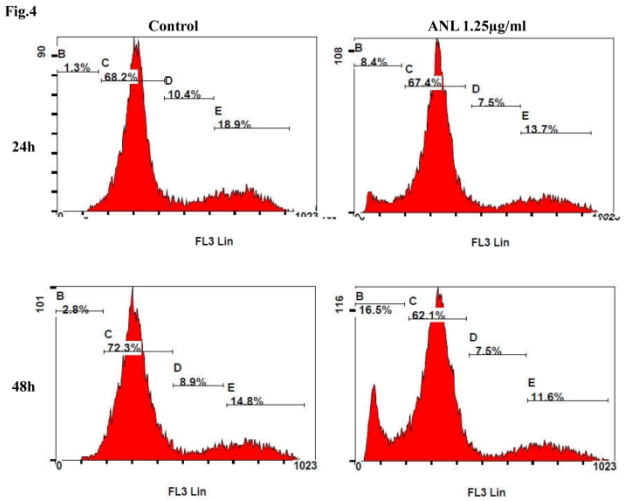

Figure 4. ANL increases hypodiploidy and decreases G0/G1 population in HepG2 cells. HepG2 cells were incubated with or without ANL (1.25 μg/mL) for either 24h or 48h. Cells were stained with propidium iodide (PI) and data acquired on the FL3 channel of the flow cytometer. B, C, D, and E represent the hypodiploid (apoptotic), G0/G1, S, and G2/M phases, respectively.

279x215mm (300 x 300 DPI)

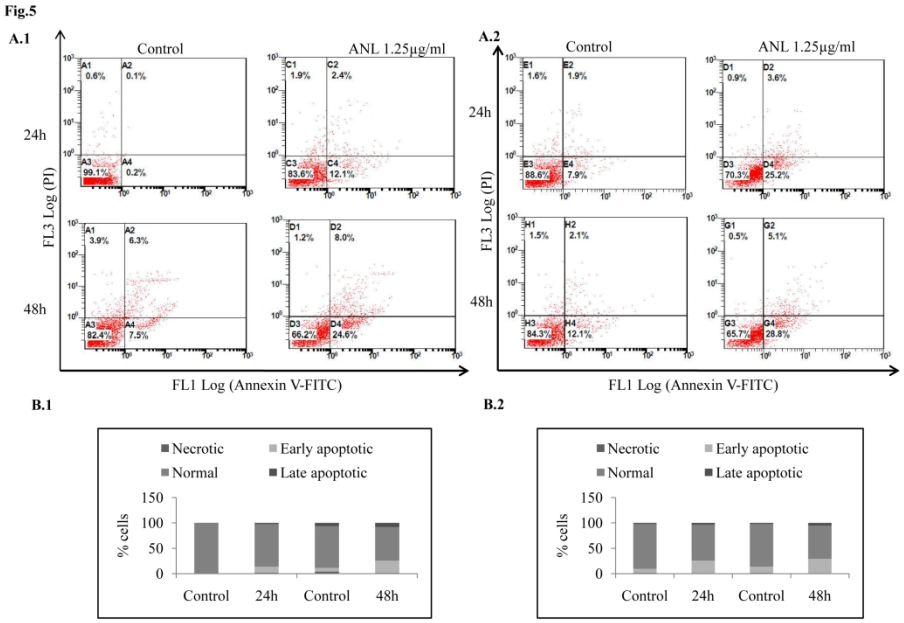

Figure 5. ANL induces apoptosis in HepG2 and HT-29 cells. HepG2 (A) and HT29 (B) cells were analysed by Annexin V/propidium iodide (PI) staining using flow cytometry. ANL (1.25 µg/mL) induced apoptosis in HepG2 cells (A.1) and HT-29 cells (B.1). The X-axis depicts Annexin V positive cells, and the Y-axis depicts PI-positive cells. A1, A2, A3 and A4 quadrants represent the necrotic, late apoptotic, normal and early apoptotic cell populations respectively, with numbers indicating the percentage number of viable, early apoptotic, late apoptotic, and necrotic cells that are present in the respective quadrants. Percentage of the cell populations in different areas are summarised in (A.2) and (B.2).

279x215mm (300 x 300 DPI)

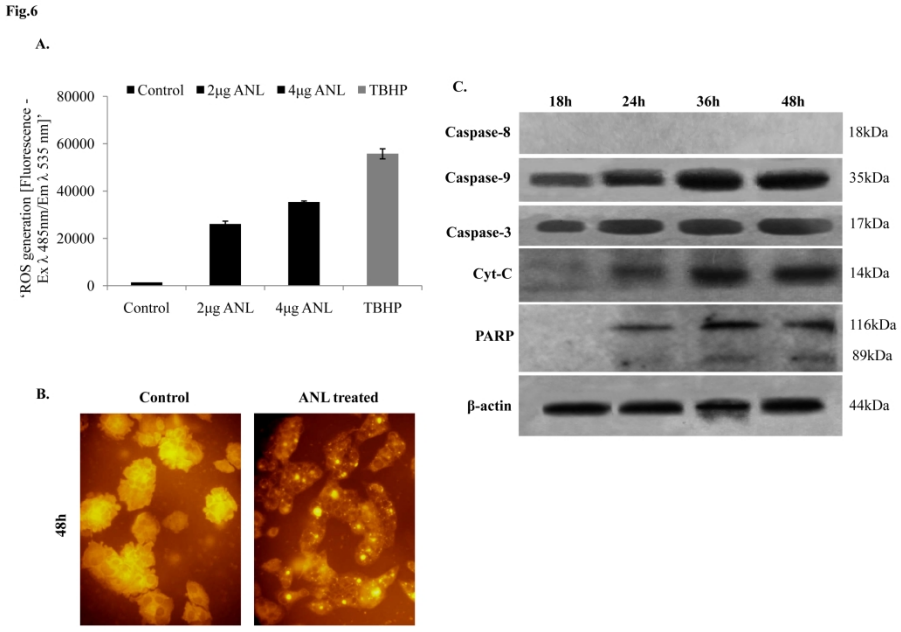

Figure 6. ANL induces oxidative stress, alters mitochondrial membrane potential and induces apoptosis in HepG2 cells. (A) Intracellular production of ROS was measured using a cell permeant fluorogenic dye 2', 7'-dichlorofluorescin diacetate (DCFDA) and fluorescence was measured by microplate reader. (B) Mitochondrial membrane potential (MMP) was measured using tetramethyl-rhodamine methyl ester (TMRM) and fluorescence microscopy. TMRM accumulates within active mitochondria of control cells (left hand panel), with ANL-inducing depolarization of mitochondrial membrane as indicated by a decrease in fluorescence (right hand panel). (C) Immunoblot analysis of activation of intrinsic apoptotic pathway in HepG2 cells treated with ANL (IC50) over 48h, indicating increased levels of caspase-3 and -9, cytochrome c and PARP-1. β-actin was used as loading control.

279x215mm (300 x 300 DPI)

Fig.7

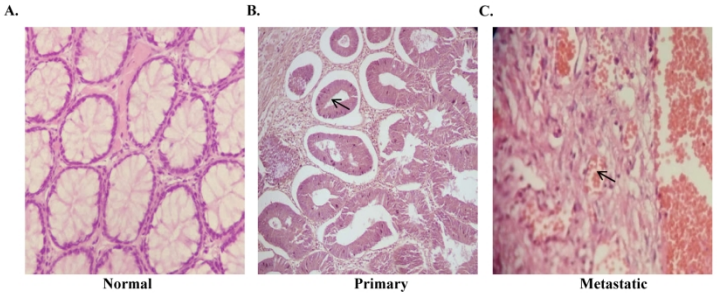

Figure 7. ANL shows differential binding to human colon cancer and normal tissues
Differential binding of ANL to normal and cancerous human colon tissues: ANL shows no binding to normal human colon tissues (A) but strong binding to primary cancer (B) and metastatic colon (C) tissues. Representative images are presented. All the images were obtained with 400X magnification. "Arrows" point to ANL binding to apical surface of the secretory gland epithelia.

279x215mm (200 x 200 DPI)

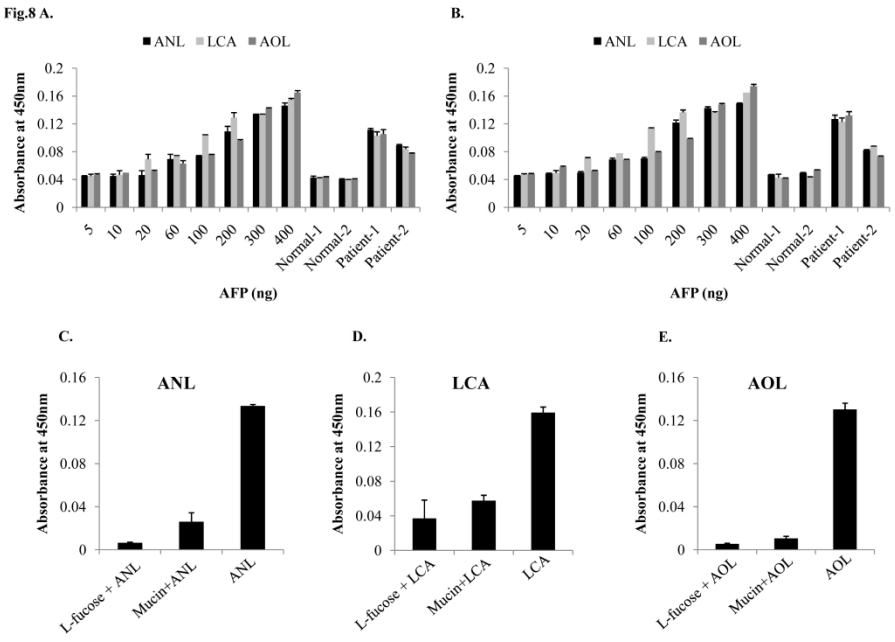

Figure 8. Sandwich ELISA using ANL and anti-AFP antibody: AFP was added in varying concentrations dissolved in PBS (A) dissolved in normal serum (B) for the standard calibration curve, and in another set the normal and HCC patient serum samples diluted 1:50 in PBS. Bound AFP antibodies were detected using HRP-conjugated secondary antibody. Absorbance was read at 450 nm. Competitive inhibition of ANL (C), LCA (D) and AOL (E) within the ELISA by competing sugar L-fucose or mucin. Both L-fucose and mucin reduced the binding of lectins to AFP (as determined by significant reduction in absorbance).

279x215mm (300 x 300 DPI)